

# Effects of Drying Process on an IgG1 Monoclonal Antibody Using Solid-State Hydrogen Deuterium Exchange with Mass Spectrometric Analysis (ssHDX-MS)

Ehab M. Moussa<sup>1</sup> · Nathan E. Wilson<sup>1</sup> · Qi Tony Zhou<sup>1</sup> · Satish K. Singh<sup>2,3</sup> · Sandeep Nema<sup>2</sup> · Elizabeth M. Topp<sup>1</sup>

Received: 21 August 2017 / Accepted: 21 November 2017 / Published online: 3 January 2018  
© Springer Science+Business Media, LLC, part of Springer Nature 2018

## ABSTRACT

**Purpose** Lyophilization and spray drying are widely used to manufacture solid forms of therapeutic proteins. Lyophilization is used to stabilize proteins vulnerable to degradation in solution, whereas spray drying is mainly used to prepare inhalation powders or as an alternative to freezing for storing bulk drug substance. Both processes impose stresses that may adversely affect protein structure, stability and bioactivity. Here, we compared lyophilization with and without controlled ice nucleation, and spray drying for their effects on the solid-state conformation and matrix interactions of a model IgG1 monoclonal antibody (mAb).

**Methods** Solid-state conformation and matrix interactions of the mAb were probed using solid-state hydrogen-deuterium exchange with mass spectrometric analysis (ssHDX-MS), and solid-state Fourier transform infrared (ssFTIR) and solid-state fluorescence spectroscopies.

**Results** mAb conformation and/or matrix interactions were most perturbed in mannitol-containing samples and the distribution of states was more heterogeneous in sucrose and trehalose samples that were spray dried.

**Conclusions** The findings demonstrate the sensitivity of ssHDX-MS to changes weakly indicated by spectroscopic methods, and support the broader use of ssHDX-MS to probe formulation and process effects on proteins in solid samples.

**KEY WORDS** conformation · interactions · lyophilization · monoclonal antibodies · spray drying

## ABBREVIATIONS

ATR	Attenuated total reflectance
BSA	Bovine serum albumin
CD	Circular dichroism
CN	Controlled ice nucleation
FTIR	Fourier transform infrared
HDX-MS	Hydrogen deuterium exchange with mass spectrometric analysis
IgG	Immunoglobulin G
$K_{fast}$	Rate of exchange of amide hydrogen atoms in the fast exchanging pool
$K_{slow}$	Rate of exchange of amide hydrogen atoms in the slow exchanging pool
mAb	Monoclonal antibody
$N_{fast}$	Number of amide hydrogen atoms in the fast exchanging pool
$N_{slow}$	Number of amide hydrogen atoms in the slow exchanging pool
PMT	Photomultiplier tube
PXRD	Powder x-ray diffraction
SD	Spray drying
SEM	Scanning electron microscope
ss	Solid-state; indicates that an analytical method has been applied to a solid sample
ssPL-MS	Solid-state photolytic labeling with mass spectrometric analysis
UNC	Uncontrolled ice nucleation

Guest Editors: Tony Zhou and Tonglei Li

**Electronic supplementary material** The online version of this article (<https://doi.org/10.1007/s11095-017-2318-9>) contains supplementary material, which is available to authorized users.

✉ Elizabeth M. Topp  
topp@purdue.edu

<sup>1</sup> Department of Industrial and Physical Pharmacy, College of Pharmacy, Purdue University, 575 Stadium Mall Drive, West Lafayette, Indiana 47906, USA

<sup>2</sup> BioTherapeutics Pharmaceutical Sciences, Pfizer Inc., Chesterfield Missouri, USA

<sup>3</sup> Present address: Lonza AG, Basel, Switzerland

## INTRODUCTION

Preserving the stability of therapeutic proteins in the final product or in bulk drug substance is critical to development. Lyophilization is the mainstay method used for producing solid forms of labile therapeutic proteins in order to improve their long-term stability (1), whereas spray drying is an alternative drying method often used to develop inhalable powders, or for bulk storage of drug substance (2).

The freeze-drying process involves freezing the protein solution and drying the frozen solid under vacuum (3). The drying step involves primary drying to sublime frozen water, followed by secondary drying to remove additional water. In the freezing step, the ice-nucleation temperature affects the size and number of ice crystals and hence affects the primary drying time (4). Ice-nucleation, however, is a stochastic process that can occur heterogeneously among the different vials in the freeze-drier. Induction of ice-nucleation at higher temperatures results in larger ice crystals (5) and reduces the area of the ice-water interface at which the protein molecule can denature. In spray drying, the protein solution is atomized into small droplets and then exposed to a drying gas at high temperature to remove water by evaporation (2). During spray drying, the protein is exposed to shear stress, air–water interfaces and extended exposure to high temperatures in the collection vessel, all of which can promote degradation (2).

The loss of hydration may disrupt the higher order structure of proteins by decreasing charge density and creating hydrophobic surfaces that facilitate aggregation (3). Accordingly, structural analysis of proteins in the solid-state is critical to the rational development of stable solid formulations (6). In dried solids, excipients are used to stabilize protein molecules against the stresses imposed by manufacturing processes and by storage conditions (7). While the effects of different excipients on the preservation of native structure in the solid-state have been studied extensively, the effects of the processing methods and conditions used to produce these solids have received relatively little attention.

Controlled ice nucleation has been shown to decrease the glycation of a model monoclonal antibody (mAb), but had no effect on structure as measured in the reconstituted solution using Fourier transform infrared (FTIR) and circular dichroism (CD) spectroscopies (8). Similarly, different primary drying rates did not affect the structure of bovine serum albumin (BSA) as measured by solid-state (ss) FTIR spectroscopy (9). The effects of different drying processes on the structure of model mAbs have also been studied by ssFTIR (10) and ssRaman (11) spectroscopies. In most cases, process effects on the physical attributes of the lyophilized cake or spray dried powder were evident, but little or no conformational change could be detected using FTIR and CD. In a recent study, Iyer *et al.* (12) showed that controlled ice nucleation did not affect the structure of myoglobin using ssFTIR and solid-state

hydrogen deuterium exchange with mass spectrometric analysis (ssHDX-MS), although minor differences in myoglobin–excipient interactions were observed using solid-state photolytic labeling with mass spectrometric analysis (ssPL-MS).

As a labeling reagent, deuterium offers the advantages of small size and high mobility, and hence may be able to detect relatively small differences in local structure and/or matrix interactions in the solid-state when monitored by mass spectrometry (13). In a separate set of studies, our group has demonstrated the utility of ssHDX-MS in detecting site-specific interactions of a model IgG1 mAb with different excipients in lyophilized solids and have shown a strong correlation with long-term storage (14). In the present study, ssHDX-MS was used to compare the effects of lyophilization with and without controlled ice nucleation, and spray drying on the conformation and matrix interactions of an IgG1 mAb formulated with sucrose, trehalose or mannitol.

## EXPERIMENTAL

### Formulation

The IgG1 mAb used in this study was a gift from Pfizer Biotherapeutics (St. Louis, MO). The protein solution was dialyzed at 4 °C into the formulation buffers (Table I) using Slide-A-Lyzer™ dialysis cassettes (Thermo Scientific, Rockford, IL). The pH was adjusted to 6.8 when necessary using phosphoric acid. Dialyzed solutions were then diluted in the respective formulation buffers to final mAb and excipient concentrations of 10 mg/mL each. mAb solutions were then filtered using Millex-GV 0.1 μm PVDF filters (Millipore, Billerica, MA). Each formulation solution was spray dried or filled into 2R vials (0.2 mL each), partially stoppered and loaded into the lyophilizer.

### Lyophilization

Lyophilization was carried out using a laboratory-scale lyophilizer (Revo®, MillRock Technology, Kingston, NY). For both the uncontrolled and controlled ice nucleation cycles, equal numbers of vials containing mAb solutions were used and surrounded by equal numbers of placebo sucrose solutions. All vials were loaded at a shelf temperature of 25 °C and equilibrated for 5 min. The shelf temperature was then ramped to 5 °C, held isothermally for 15 min, then ramped to –5 °C and held isothermally for 15 min. To induce controlled ice nucleation, 15 mL of de-ionized distilled water were spiked as an ice-fog into the chamber at 2 mL/min using a FreezeBooster™ unit (MillRock Technology) at the end of the isothermal hold at –5 °C. For the freezing step in both cycles, the shelf temperature was ramped to –40 °C and held isothermally for 60 min. For primary drying, the temperature was

**Table 1** Formulations Composition and Moisture Content

Formulation <sup>a</sup>	Excipient	Moisture content (w/w) <sup>b</sup>	Moisture content at 11%RH <sup>b,c</sup>
S-UCN	Sucrose	1.10 ± 0.03	2.53 ± 0.45
S-UCN-H	Sucrose	10.6 ± 2.03	NM
S-UCN-G	Sucrose	1.10 ± 0.03	NM
S-CN	Sucrose	1.43 ± 0.42	2.96 ± 1.07
S-SD	Sucrose	1.48 ± 0.42	NM
S-SDND	Sucrose	9.34 ± 2.25	6.29 ± 0.22
T-UCN	Trehalose	1.00 ± 0.21	3.33 ± 0.58
T-UCN-H	Trehalose	12.4 ± 2.84	NM
T-CN	Trehalose	1.64 ± 0.69	3.45 ± 0.39
T-SD	Trehalose	1.3 ± 0.1	NM
T-SDND	Trehalose	10.4 ± 1.3	6.94 ± 1.66
M-UCN	Mannitol	0.83 ± 0.21	1.75 ± 0.47
M-CN	Mannitol	0.9 ± 0.01	1.59 ± 0.36
M-SD	Mannitol	1.40 ± 0.27	NM
M-SDND	Mannitol	8.88 ± 0.41	5.50 ± 0.18

<sup>a</sup>All formulations were dried from solutions that initially contained 10 mg/mL protein and 10 mg/mL excipient in 2.5 mM potassium phosphate buffer, pH 6.8. UCN, uncontrolled ice nucleation. CN, controlled ice nucleation. H, hydrated at 43% RH for 30 and 60 min. G, lyophilized cake ground using a mortar and pestle. SD, spray dried, SDND, spray dried and not dried under vacuum. S, sucrose, T, trehalose, M, mannitol

<sup>b</sup>Residual moisture content measured by Karl Fischer titration. Values represent the mean ± SEM (n = 2)

<sup>c</sup>Moisture content in samples incubated at 11%RH for 10 days. NM = not measured

ramped to -35 °C and held isothermally for 24 h at a chamber pressure of 70 mTorr. The end of primary drying was determined by the convergence of the pressure readings of the Pirani and capacitance manometer gauges. For secondary drying, the temperature was ramped to 25 °C and held isothermally for 12 h at a chamber pressure of 70 mTorr. For the hydration experiment, lyophilized samples were placed uncapped in a desiccator containing a saturated solution of KCl in water (~43% RH) at room temperature for 30 and 60 min.

### Spray Drying

Spray drying was carried out using a laboratory scale spray dryer (Mini Spray Dryer B-290, Büchi, New Castle, DE). A liquid feed flow rate of 2 mL/min and an air volumetric flow rate of 600 L/min were used, with inlet and outlet temperatures of 100 and ~54 °C, respectively. The collected powder was distributed into 2 mL vials and further dried in a lyophilizer for 24 h at 30 °C and 100 mTorr to decrease the moisture content to about 2%, in order to ensure that the lyophilized and spray dried samples would be compared at similar moisture content. Due to the large volume of protein solution required for spray drying, each formulation was run only once.

### X-ray Powder Diffraction

X-ray powder diffraction (PXRD) analysis of the lyophilized and spray dried powders was conducted using a Rigaku

SmartLab X-ray diffractometer (Rigaku, The Woodlands, TX) equipped with Cu K $\alpha$  X-ray source and Bragg–Brentano geometry. The lyophilized cakes were pulverized and powder was placed on a glass slide and loaded onto the slide-holder. The spray dried powders were loaded without any processing. Diffraction intensity was obtained as a function of 2 $\theta$  values measured between 5 and 40 degrees with a step size of 0.04° at a scan rate of 40°/min.

### Scanning Electron Microscopy

The presence of crystals in the lyophilized and spray dried mannitol formulations was visualized using scanning electron microscopy (SEM). Powders were mounted on a sample holder and sputter-coated with carbon graphite. Images were obtained using a Nova NanoSEM 200 system (Fei, Hillsboro, Oregon) in 5 kV mode.

### Karl Fischer Titration

The residual moisture content in the lyophilized and spray dried powders was determined by Karl Fischer titration using 831 KF Coulometer (Metrohm, Riverview, FL). Lyophilized cakes or spray dried powders in 2 mL vials were reconstituted with 1 mL of Hydranal®-methanol dry (Fluka, St. Louis, MO) and the suspension was then injected into the cell and titrated with the Riedel-de Haën Hydranal® Coulomat reagent

(Hoechst Celanese Corp., Germany) until the end point was reached. For each formulation, 2 vials were analyzed.

### Solid-State Fourier Transform Infrared Spectroscopy

ssFTIR measurements were performed in attenuated total reflectance (ATR) mode using a Nicolet Nexus spectrometer (Thermo Scientific, Waltham, MA) equipped with a Smart iTR accessory. For the solid samples, powder was loaded and pressed against the diamond using a metal anvil. Spectra were collected in absorbance mode from 800 to 4000  $\text{cm}^{-1}$  (120 scans and 4  $\text{cm}^{-1}$  resolution). Collected spectra were processed (baseline-correction, smoothing, normalizing and second derivatization) using OPUS 6.5 software (Bruker, Billerica, MA).

### Solid-State Fluorescence Spectroscopy

Solid-state intrinsic fluorescence measurements were performed in front surface mode using a Cary-Eclipse spectrofluorometer (Agilent, Santa Clara, CA). Spray dried powders or pulverized lyophilized cakes were loaded into the solid-state sample holder and pressed so that the fused silica plate was completely covered with powder. Spectra were collected using an incident angle of 25 degrees, slit width of 5 nm and a photomultiplier tube (PMT) voltage of 600. The samples were excited at 280 nm and the emission spectra were collected from 280 to 450 nm. Collected spectra were intensity-normalized.

### Solid-State Hydrogen Deuterium Exchange with Mass Spectrometric Analysis (ssHDX-MS)

Vials containing lyophilized cakes or spray dried powders were placed in a sealed desiccator at 22°C containing a  $\text{D}_2\text{O}$  solution saturated with LiCl to produce the equivalent of 11% RH in  $\text{D}_2\text{O}$ . For each formulation, 3–5 vials were removed after 4, 12, 24, 48, 120 and 240 h of exposure to  $\text{D}_2\text{O}$  vapor. At each time point, deuterium exchange was stopped by rapidly cooling the vials by placing them on dry-ice and then storing at  $-80^\circ\text{C}$ . To analyze deuterium incorporation, the samples were reconstituted in 2 mL ice-cold 0.1% formic acid (FA) at pH  $\sim 2.5$  and 10  $\mu\text{L}$  were injected onto a protein microtrap (Michrom Bioresources, Inc., Auburn, CA). The samples were desalted for 1.7 min with 10% acetonitrile, 90% water and 0.1% FA and eluted over 7 min and a gradient of 90% acetonitrile, 10% water, and 0.1% FA using high performance liquid chromatography (1200 series, Agilent Technologies, Santa Clara, CA). All columns were housed in a custom-built refrigeration unit kept at  $\sim 0^\circ\text{C}$  to minimize hydrogen back exchange. Mass spectra were acquired by a 6520 qTOF mass spectrometer (Agilent Technologies, Santa Clara, CA) in the extended mass range

(200–20,000  $m/z$ ), and the masses of the undeuterated and deuterated mAb were obtained by deconvoluting the acquired spectra using the maximum entropy function of the MassHunter Workstation Software version B.04 (Agilent Technologies). The deconvolution algorithm converts mass envelopes detected for various charge states to the actual mass values of the different species in the sample.

### Hydrogen Deuterium Exchange Data Analysis

The kinetics of hydrogen-deuterium exchange as a function of time was fitted to a bi-exponential association model:

$$D(t) = N_{fast}(1 - e^{-k_{fast}t}) + N_{slow}(1 - e^{-k_{slow}t}), \quad (1)$$

where  $D(t)$  is number of deuterons taken up at time  $t$ ,  $N_{fast}$  and  $N_{slow}$  are the numbers of amide hydrogen atoms in the rapidly and slowly exchanging pools, respectively, and  $k_{fast}$  and  $k_{slow}$  are the respective exchange rate constants.

Deconvoluted and normalized mass envelopes for deuterated samples were compared and used as a measure of differences in structure and/or matrix interactions induced by the different processing methods. For this analysis, the deconvoluted mass spectra were normalized to the same arbitrary intensity and the areas of the normalized mass envelopes were calculated using Prism Software (GraphPad, La Jolla, CA).

## RESULTS

### Effect of Controlled Ice Nucleation on Primary Drying Time

The end point of primary drying in the lyophilization cycles was determined by the convergence of the readings of the Pirani and capacitance manometer pressure gauges. The use of the ice-fog method to induce ice nucleation in all vials at  $-5^\circ\text{C}$  decreased the primary drying time from 13 to 11 h (Fig. S1). While this margin is small in absolute terms, it represents a 15% reduction in drying time. Here, it is important to note that the fill volume is small ( $\sim 0.2$  ml) and the load size is only half a shelf. The absolute reduction in drying time would be expected to be greater for larger fill volumes and shelf loads.

### Effect of Formulation and Process on Moisture Content and Crystallinity

For each formulation composition, moisture content was slightly greater in samples lyophilized using controlled ice nucleation (CN) than in those lyophilized with uncontrolled ice nucleation (UCN) (Table I). Among the lyophilized

formulations, mannitol retained the least amount of moisture followed by sucrose and then trehalose. The moisture content in the lyophilized formulations hydrated for 30 and 60 min was 10–12%. In all lyophilized formulations that were not hydrated, the moisture content was less than 4% (*w/w*) after 10 days of incubation under D<sub>2</sub>O vapor at 11%RH and 22 °C.

The spray dried formulations had significantly greater moisture content than their lyophilized counterparts, but less than the hydrated lyophilized samples. Further drying of the spray dried samples under vacuum at 30 °C reduced the moisture content to levels similar to those of the lyophilized samples. The spray dried mannitol formulation retained the least amount of moisture followed by sucrose and then trehalose. Incubating the high-moisture content spray dried formulations for 10 days under D<sub>2</sub>O vapor at 11%RH and 22 °C resulted in the loss of about 3% (*w/w*) of the original moisture content.

All sucrose and trehalose formulations prepared by all processes were completely amorphous as measured by PXRD (Fig. S2). For the mannitol formulations, minor crystalline peaks in the M-SD and M-UCN formulations were observed by PXRD, whereas M-CN was completely amorphous. Using SEM, crystallinity was observed in M-SD and M-UCN samples, but not in M-CN (Fig. 1). Additionally, sharp peaks were observed in the fingerprint (800–1200 cm<sup>-1</sup>) and C-H stretching regions (2800–3200 cm<sup>-1</sup>) of the ssFTIR spectra of M-SD samples, consistent with crystallinity, whereas less sharp and completely broad peaks were observed in M-UCN and M-CN samples, respectively (Fig. S2). Taken together, the results from PXRD, SEM and FTIR indicate that mannitol is partially crystalline in M-SD and M-UCN and completely amorphous in M-CN. Although crystallization was not evaluated after exposure of the cakes to 11%RH at 22 °C, in a previous report from our laboratory, exposing similar preparations of 1:1 protein:mannitol ratio to 11%RH and 23 °C did not induce mannitol crystallization (15). Such lack of mannitol crystallinity is likely due to the inhibition thereof by the amorphous mAb phase that constitutes 50% of the formulation components by weight. Microphase separation of mannitol cannot be ruled out, however.

### Secondary Structural Analysis Using ssFTIR

The peaks in the Amide I region of ssFTIR spectra of the mAb formulations were in general agreement with typical FTIR spectra reported for IgG (16), with bands at ~1615 cm<sup>-1</sup> ( $\beta$ -sheet or side chain), ~1637 cm<sup>-1</sup> ( $\beta$ -sheet), ~1661 and ~1677 cm<sup>-1</sup> (turns), and ~1690 cm<sup>-1</sup> ( $\beta$ -sheet) (Fig. 2). Among the spectra recorded for the various formulations and drying processes, differences were observed only in the major  $\beta$ -sheet peak at ~1637 cm<sup>-1</sup> (Fig. 2). For all three

excipients, SDND samples showed a decrease in peak intensity compared to UCN, CN and SD formulations (Fig. 2). The M-SDND formulation showed the largest decrease (Fig. 2c) followed in order by T-SDND (Fig. 2b) and S-SDND (Fig. 2a). The spectra for the sucrose formulations (S-UCN, S-CN and S-SD) were nearly identical (Fig. 2a), whereas for the trehalose formulations, the peak intensity was slightly lower in T-CN and T-SD than in T-UCN (Fig. 2b). For the mannitol formulation, the peak intensity in M-SD was less than in M-UCN and M-CN (Fig. 2c).

The recovery of secondary structure in the different formulations after reconstitution was evaluated using far-UV CD spectroscopy. The spectra of protein solutions prior to drying had a minimum at 218 nm and a maximum at 201 nm, consistent with a  $\beta$ -sheet dominated structure (Fig. S4) (17). For all formulations and drying methods, minor changes in peak intensity but no changes in peak positions were observed, indicating that changes in the secondary structure observed in the solid-state were reversible upon reconstitution.

### Tertiary Structural Analysis Using Intrinsic Fluorescence

To further understand structural differences among the various solids, intrinsic fluorescence measured in front surface mode was employed. In the solid-state, the fluorescence maximum is typically blue-shifted by approximately 20 nm compared to aqueous solution due to the greater hydrophobicity associated with dehydration (18). The fluorescence maximum of a fully exposed tryptophan residue in the solid-state was determined to be approximately 334 nm (19). In the discussion that follows, changes in peak intensity are not considered because concentration dependence is unlikely in the solid-state (18).

For all processes, no changes in peak position were detected in the sucrose and trehalose formulations (Fig. 3a–b). In contrast, in M-SD the peak was redshifted by ~3 nm relative to M-CN and M-UCN (Fig. 3c) indicating a change in the local environment of the tryptophan side chain. Notably, M-SD had similar moisture content to S-CN, S-SD, T-CN and T-SD, suggesting that the observed red-shift is due to partial unfolding rather than hydration. Intrinsic fluorescence maxima measured in solution after reconstitution were identical in all formulations (Fig. S5), indicating that the change observed in the solid-state is reversible.

### Structural Analysis Using Hydrogen-Deuterium Exchange

Deuterium uptake as a function of time in the solid formulations was monitored as a measure of protein conformation and matrix interactions. In ssHDX, the rate of exchange can be affected by the rate of moisture sorption, the mass transport



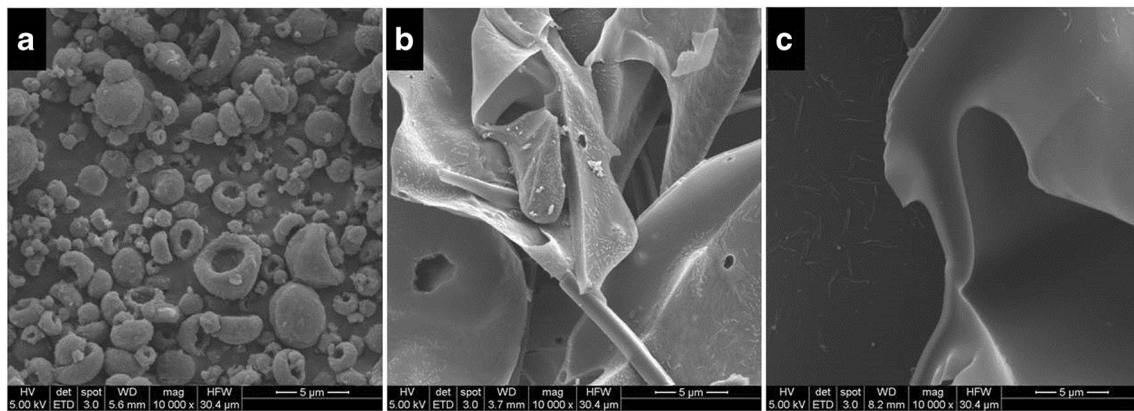


**Fig. 1** Scanning electron micrographs of mannitol formulations. **(a)** Spray dried (M-SD, Table I). **(b)** Lyophilized with uncontrolled ice nucleation (M-UCN, Table I). **(c)** Lyophilized with controlled ice nucleation (M-CN, Table I). The rough surfaces in **(a)** and **(b)** represent crystallization of mannitol.

of  $D_2O$  vapor through the solid sample, the hydrogen-bond network experienced by the protein in the solid matrix (i.e., intermolecular hydrogen bonds), and by the folded-state of the protein (i.e., intramolecular hydrogen bonds). Moisture sorption in lyophilized formulations similar to those used in this study (15) is typically complete within 1 h, so it is reasonable to assume that moisture sorption kinetics affects deuterium uptake only during the first few hours of the ssHDX experiment.

For spray dried samples, mass transport through the dense powder may slow ssHDX kinetics when compared to the lyophilized cakes. To explore mass transport effects, we measured ssHDX kinetics in lyophilized sucrose formulations that were ground after lyophilization (S-UCN-G) to produce a denser powder. The rate of ssHDX in this formulation was initially slower than that in intact cakes until the two curves become coincident at  $\sim 48$  h (Fig. 4a), suggesting completion of any mass transport effects. This indicates that ssHDX

kinetics at early time points can be obscured by powder compactness, but, it is unlikely that mass transport affects the extent of ssHDX on comparing spray dried powders and lyophilized cakes up to 10 days.

The high moisture content typical of spray dried samples may also obscure comparison with the lower moisture content lyophilized formulations. Accordingly, the spray dried formulations were subjected to additional drying under vacuum to reduce the moisture content to a level similar to that of the lyophilized formulations. Indeed, for all excipients, the higher moisture content spray dried formulations (SDND) incorporated more deuterium than those further dried under vacuum (Fig. 4). As a result, ssHDX in lyophilized formulations was compared to the low moisture content spray dried samples (SD).

For each formulation composition, the extent of ssHDX was used as a measure of the effect of the different drying processes on the folding state and/or the extent of interactions

**Fig. 2** ssFTIR spectra in the Amide-I region of various lyophilized and spray dried mAb formulations containing **(a)** sucrose, **(b)** trehalose or **(c)** mannitol (see Table I for composition). UCN, lyophilized with uncontrolled ice nucleation. CN, lyophilized with controlled ice nucleation. SD, spray dried with further drying under vacuum. SDND, spray dried without further drying under vacuum. S, sucrose. T, trehalose. M, mannitol.

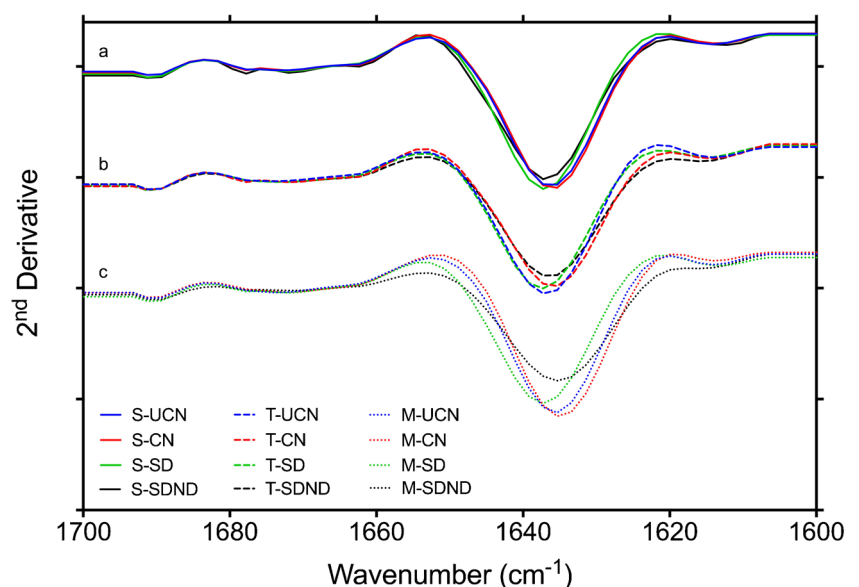
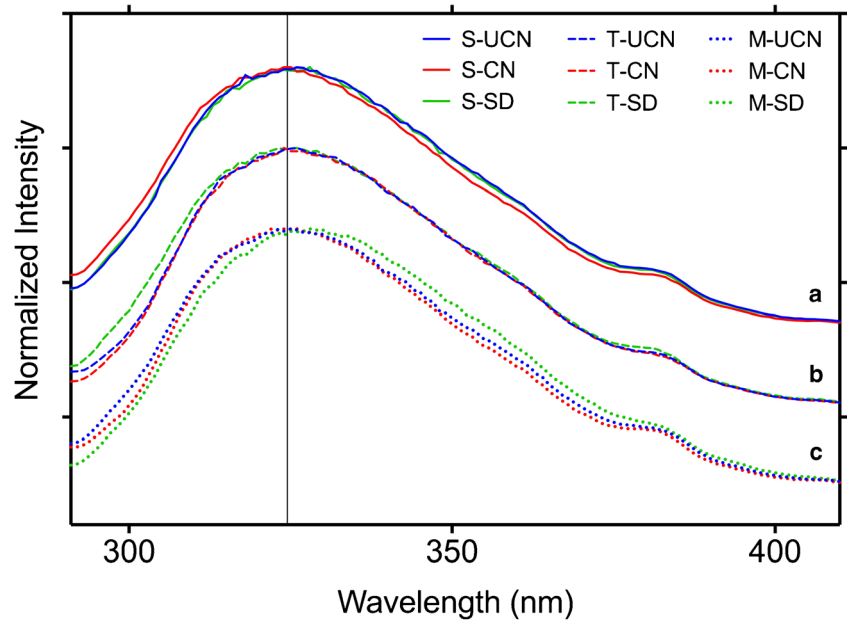


**Fig. 3** Solid-state intrinsic fluorescence spectra of various lyophilized and spray dried mAb formulations containing (a) sucrose, (b) trehalose or (c) mannitol (see Table 1 for composition). UCN, lyophilized with uncontrolled ice nucleation. CN, lyophilized with controlled ice nucleation. SD, spray dried with further drying under vacuum. S, sucrose. T, trehalose. M, mannitol. The vertical line corresponds to the maximum in fluorescence intensity at 325 nm.



of the mAb with the excipients. After 10 days of exposure to  $D_2O$ , the extent of ssHDX was similar in S-UCN and S-CN samples, and in T-UCN compared to T-CN samples, but was slightly less in M-CN than in M-UCN samples (Fig. 5). Interestingly, the extent of ssHDX was less in S-SD than in S-CN or S-UCN samples, but was comparable in T-SD, T-UCN and T-CN samples. This is consistent with results for sucrose formulations of other therapeutic proteins (unpublished data). In contrast to sucrose, the extent of ssHDX was greater in M-SD than in M-UCN and M-CN samples.

In S-SD and T-SD samples, spectra were unusually broadened compared to their lyophilized counterparts (Fig. 6),

suggesting that the ensemble of protein conformations and/or matrix interactions in these samples is more heterogeneous than in the samples produced by lyophilization. Peaks at similar percentages of deuterium uptake ( $\sim 15\%$  for sucrose,  $\sim 17\%$  for trehalose and  $\sim 23\%$  for mannitol) were selected to demonstrate the broadening effect (Fig. 6). Well resolved peaks were obtained in the back exchanged S-SD and T-SD samples (Fig. 6e), indicating that the observed broadening is not due to glycan degradation. Moreover, well resolved peaks were obtained in the hydrated lyophilized samples (S-UCN-H and T-UCN-H), which excludes the role of moisture in the observed broadening (Fig. 6b–c).

**Fig. 4** Kinetics of solid-state hydrogen-deuterium exchange (ssHDX) in solid samples containing: (a, b) sucrose, (c) trehalose or (d) mannitol and prepared using lyophilization with uncontrolled ice nucleation (UCN), lyophilization with controlled ice nucleation (CN) or spray drying with further drying under vacuum (SD). Symbols represent the average increase in mass (Da) at each time point; lines represent the best-fit line obtained using Eq. 1. S, sucrose. T, trehalose. M, mannitol. G, ground lyophilized cake.

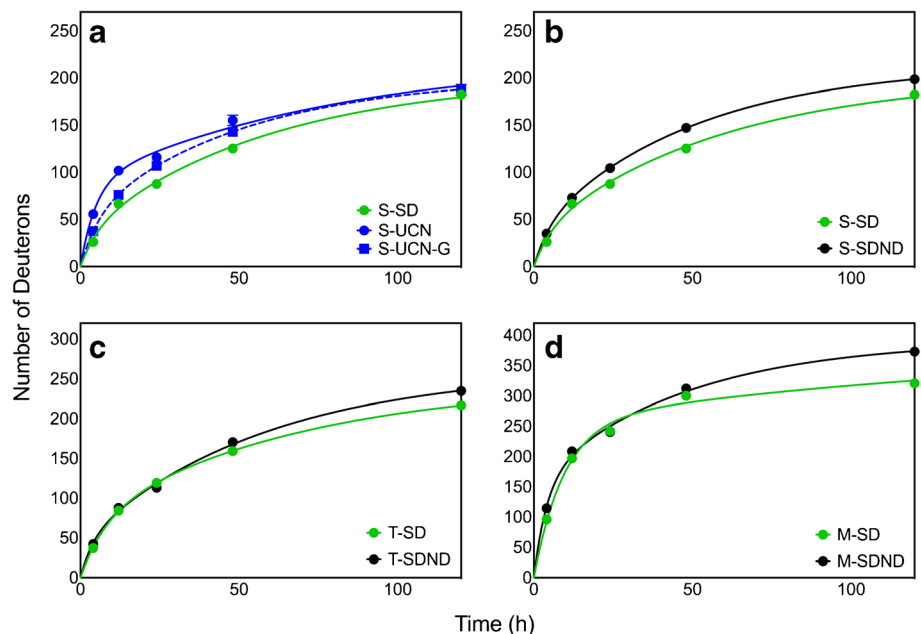
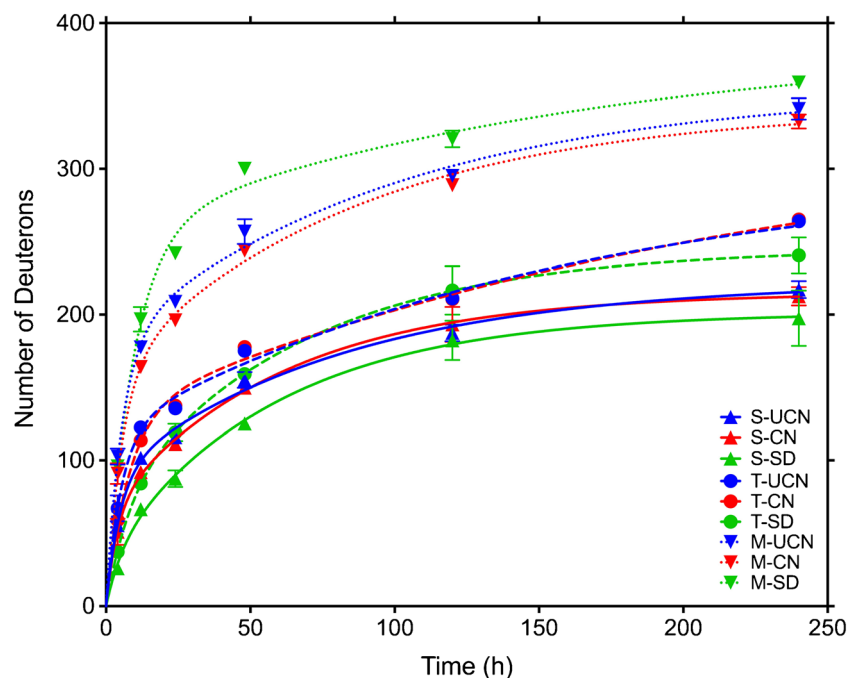


**Fig. 5** Solid-state hydrogen-deuterium exchange (ssHDX) kinetics. S, sucrose. T, trehalose. M, mannitol. UCN, uncontrolled ice nucleation lyophilization cycle. CN, controlled ice nucleation lyophilization cycle. SD, spray drying with further drying under vacuum. Symbols represent the average increase in mass (Da) at each time point. Lines represent the best-fit obtained using Eq. 1.



The mAb studied here has three dominant glycoforms differing from one another by  $\sim 160$  Da, which corresponds to galactose (Fig. 6a). Since baseline resolution of the three peaks could not be achieved, peak widths could not be used to compare the broadness of the mass envelopes. Because broadening of the peaks in the deconvoluted spectra is expected to decrease resolution of the glycoform peaks and increase peak area, the areas under the curve (AUC) of the intensity-normalized deconvoluted spectra were used as a measure of peak broadening (Figs. 6 and 7).

In general, the resolution of the glycoforms decreased with increased deuterium uptake and was nearly lost in a deuterated solution control denatured with guanidine hydrochloride (Fig. 6a). For formulations containing sucrose or trehalose, UCN samples had the smallest AUC followed in order by CN and SD (Fig. 6b–c). This suggests that, among the three processing methods, spray drying produced solids in which the mAb structure and/or matrix interactions are the most heterogeneous. For the mannitol formulation, however, peak broadening beyond that in the native solution controls was greater in M-UCN and M-CN samples than in M-SD (Fig. 6d), indicating that heterogeneity in structure and/or matrix interactions was greatest for samples dried using lyophilization when mannitol is used as the excipient.

Additionally, in S-SD and T-SD samples, broadening was associated with minor splitting of the glycoform peaks (Fig. 6b–c), which suggests the presence of two distinct populations differing in structure and/or the extent of interactions with the matrix. Interestingly, the AUC of the guanidine control sample, which is relatively highly deuterated ( $\sim 43\%$ ), was comparable to those of the  $\sim 20\%$  deuterated sucrose and trehalose

formulations (Fig. 7a–b), consistent with comparable heterogeneity.

To gain further insights into peak broadening, peak areas were plotted as a function of the percentage of deuterium uptake (Fig. 7). The average peak area of the native solution control was  $\sim 78\%$  (Fig. 7, dotted line) with a standard deviation of  $\sim 1\%$  (Fig. 7, dashed lines). At high levels of deuterium uptake, peaks broadened beyond the effect of deuterium incorporation observed in the native solution control, suggesting spatial and/or conformational heterogeneity. For the sucrose formulations, the AUC was consistently largest in SD samples followed in order by CN and UCN samples (Fig. 7a). For the trehalose formulations, the differences between the three curves narrowed as the percentage of deuteration increases, converging at  $\sim 17\%$  deuterium uptake (Fig. 7b). The rank order of the curves (SD > CN > UCN) is similar in the sucrose and trehalose formulations (Fig. 7a–b) although the difference between UCN and CN formulations is much smaller in the trehalose formulation.

The curves for the mannitol formulation were similar to those for sucrose and trehalose in UCN and CN samples (Fig. 7). For M-SD samples, however, smaller AUCs were observed at high deuterium uptake relative to M-UCN and M-CN. Also, no peak splitting was observed in any mannitol sample. Notably, the AUCs in all mannitol samples were less than those in trehalose and sucrose formulations, suggesting a more homogenous distribution of conformations, and/or matrix interactions or the lack thereof (Fig. 7). That mannitol formulations were significantly more deuterated suggests that, while the structure and matrix interactions may be more



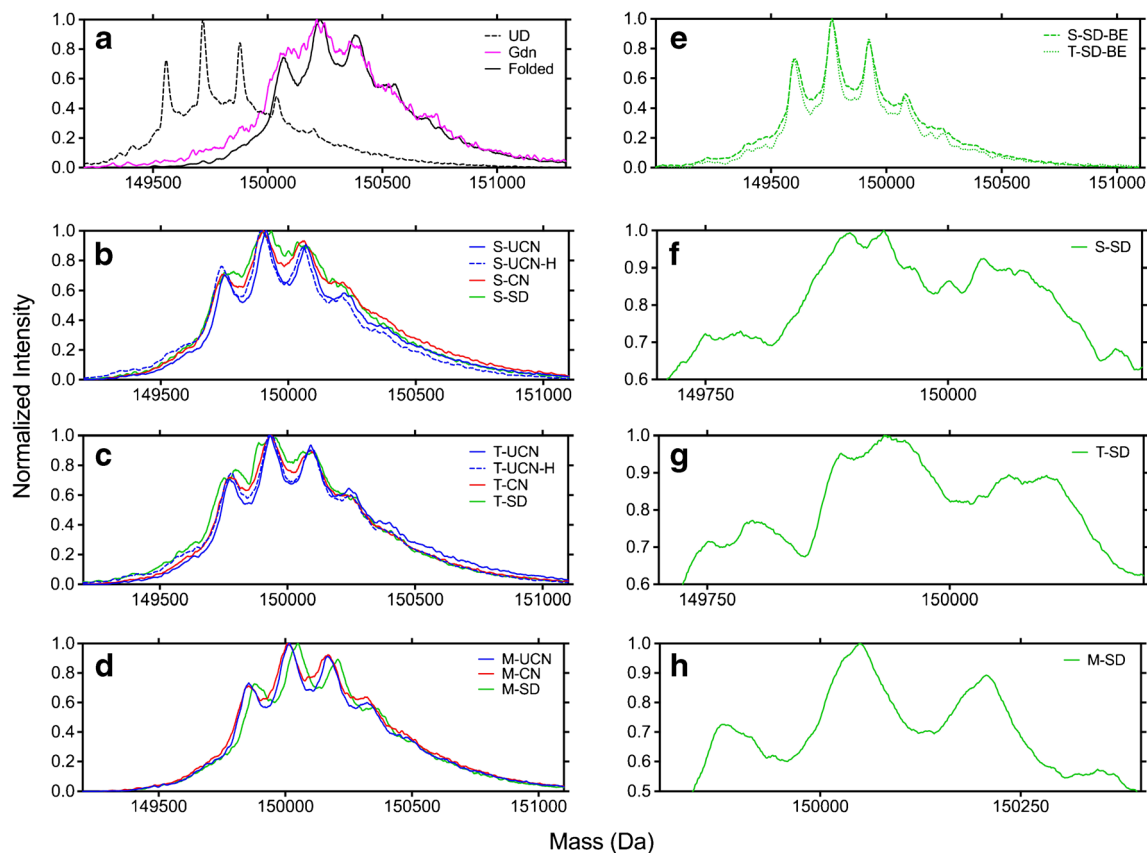


**Fig. 6** Deconvoluted mass spectra of lyophilized and spray dried mAb samples from ssHDX-MS studies compared with solution controls. **(a)** Solution controls: native mAb in solution prior to deuterium exposure (“undeuterated”, UD; negative control) and following exposure to D<sub>2</sub>O or to both Gdn HCl and D<sub>2</sub>O to generate a denatured and deuterated sample. Panels **(b–d)** show spectra of solid samples subjected to ssHDX-MS after drying using lyophilization with uncontrolled ice nucleation (UCN), lyophilization with controlled ice nucleation (CN), spray drying with further drying under vacuum (SD) or lyophilized formulations hydrated by incubation at 43% relative humidity for 30 min (UCN-H); see text for process details. Panel **(e)** shows spectra of the back-exchanged spray dried sucrose and trehalose formulations (S-SD-BE and T-SD-BE, respectively). Panels **(f–h)** show a zoomed-in view of the peaks in SD formulations. Each panel corresponds to a particular formulation, **(b and f)** sucrose, **(c and g)** trehalose, **(d and h)** mannitol; see Table 1 and text for formulation compositions.

homogenous, the mAb is also more exposed, suggesting fewer intra- and intermolecular hydrogen bonds (Figs. 5 and 7).

## DISCUSSION

Over the past few decades, the effects of formulation composition on the structure of lyophilized and spray dried proteins has been the subject of numerous studies (11,20–23). Comparatively few studies have addressed the effects of the different manufacturing processes, however (10,11). In the present study, the effects of lyophilization with controlled ice nucleation, lyophilization without controlled ice nucleation, and spray drying on the structure and matrix interactions of an IgG1 mAb were compared using ssHDX-MS and various orthogonal methods. While our group has explored the effects of lyophilization with and without controlled ice nucleation on lyophilized myoglobin using ssHDX-MS in the past (12), to our knowledge this is the first study to address the effects of spray drying using this method.

In HDX-MS analysis of proteins, the rate of exchange of amide hydrogen atoms is measured by using quench conditions that slow back exchange of amide deuterium atoms; back exchange for protein side chains and excipients are too rapid to allow their deuteration state to be measured. Thus, the extent of deuterium uptake in the solid-state can be taken as a measure of the intra- and intermolecular hydrogen-bonding interactions that the protein experiences in the solid matrix. As intramolecular hydrogen bonds contribute to the folded structure of proteins, a less fully folded protein in the solid-state would be more “exposed” to D<sub>2</sub>O sorbed into the solid from the vapor phase, and would incorporate a greater number of deuterons via exchange reactions at the exposed amide groups. This aspect of ssHDX is analogous to solution HDX, in which deuterium incorporation reflects, in part, the degree of protein folding. In ssHDX, however, the extent of deuterium incorporation may also depend on intermolecular hydrogen bonds between the protein molecule and neighboring components of the solid, which may include excipients, residual water or other protein molecules. Sorbed D<sub>2</sub>O must

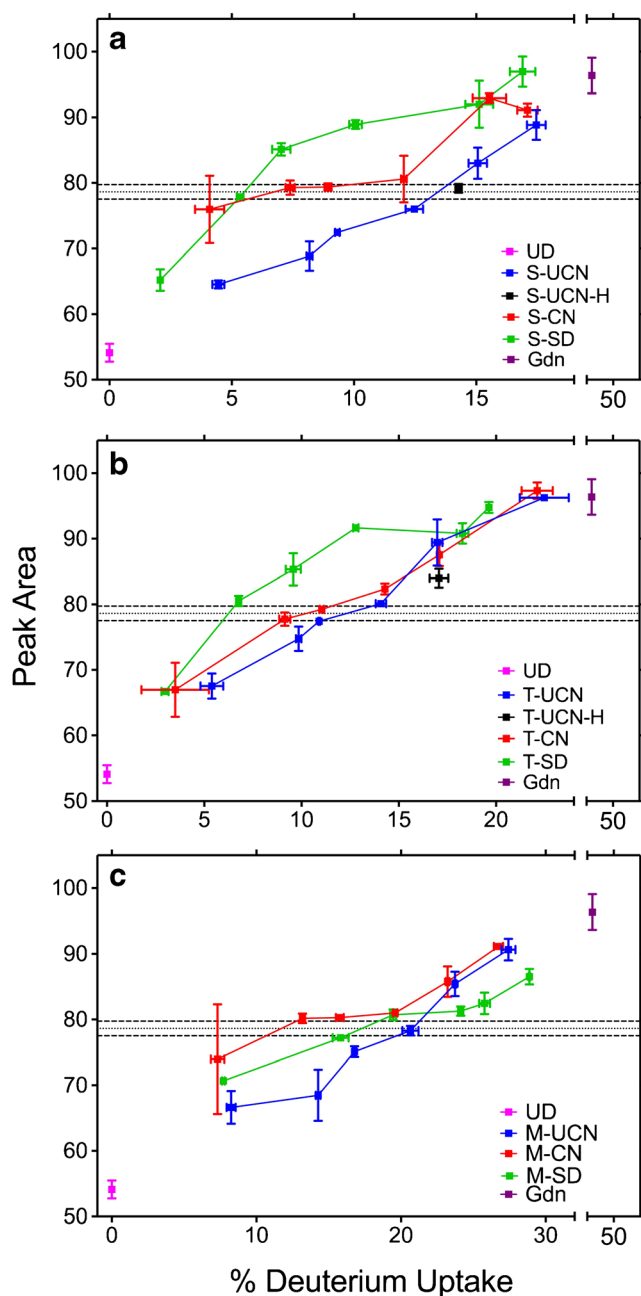


**Fig. 7** Peak areas of the deuterated mass envelopes as a function of deuterium incorporation for lyophilized and spray dried mAb samples subjected to ssHDX-MS, compared with solution controls. Peak areas are reported as a percentage of greatest peak area measured, i.e., in the guanidine control sample. Panels (a–c) show results for samples dried using lyophilization with uncontrolled ice nucleation (UCN), lyophilization with controlled ice nucleation (CN), or spray drying with further drying under vacuum (SD); see text for process details. Each panel corresponds to a particular formulation: (a) sucrose, (b) trehalose or (c) mannitol; see Table 1 and text for formulation compositions. Individual points correspond to different times during the deuteration time course. The horizontal dotted line represents the average peak area of the native solution control samples deuterated for 30, 60, 120 or 180 min. Dashed lines represent 1 standard deviation of the average peak area of the native solution controls ( $n = 4$ ). Error bars represent the standard deviation of the mean of each formulation at each time point ( $n = 2–3$ ).

compete with both intra- and intermolecular hydrogen bonds to initiate exchange in ssHDX. Simplistically, then, protection from exchange in the solid-state (i.e., the difference between the theoretical number of exchangeable amide hydrogens and the number of deuterons incorporated in ssHDX) represents the sum of the intra- and intermolecular hydrogen bonds that are of sufficient strength to resist competition by sorbed  $D_2O$ .

In the ssHDX studies reported here, deuterium incorporation in S-SD samples was less than in S-UCN and S-CN samples (Fig. 4). No structural changes of the mAb in these formulations were observed by ssFTIR and solid-state fluorescence spectroscopies, however. This is consistent with the results by Sane *et al.* (11), in which the structure of a model mAb was similarly retained in spray dried and lyophilized formulations containing sugars, but is in contrast with the results by Abdul-Fattah *et al.* (10), in which spray dried sucrose formulations of a model mAb retained more native-like secondary structure than lyophilized ones but exhibited more mobility. Taken together, the extent of ssHDX and spectroscopic results in the present study suggest that the slight protection from ssHDX in S-SD samples may be due to greater mAb-sucrose interactions in the spray dried powder than in the lyophilized cakes, rather than to a more folded state. One possible reason for this could be that sucrose molecules are better arranged around the mAb molecule as water evaporates from the atomized droplets compared to when ice crystals sublime during lyophilization. Alternatively, ssHDX may be sensitive to structural changes that are undetected by ssFTIR and solid-state fluorescence spectroscopies.

In contrast to the results with sucrose, the extent of ssHDX in M-SD samples was greater than in M-CN and M-UCN samples (Fig. 4). In M-SD samples, limited mannitol-mAb interactions are expected due to the partial crystallinity of mannitol. This difference in the extent of interactions is evident in the fingerprint and C-H stretch regions of the ssFTIR spectra (Figure S3), where the sharp peaks in M-SD samples indicate few or no interactions, whereas the broader peaks in M-UCN and M-CN indicate the presence of mannitol-mAb interactions. Increased deuterium uptake in M-SD samples may also be due to partial unfolding as measured by solid-state fluorescence spectroscopy.

The kinetics of HDX in solution are usually interpreted according to the Linderstrom-Lang scheme (24). In this model, hydrogen bonds involving the peptide bonds in the folded structure are transiently disrupted by local or global unfolding, with the chemical exchange reaction then occurring at solvent exposed peptide bonds on the protein surface or exposed through transient unfolding. Experimentally, the kinetics of solution HDX is often well described by a bi-exponential equation of the form of Eq. 1, a form that we have also applied successfully to ssHDX of solid samples both here and elsewhere (25–27). For solid samples, the fundamental processes that give rise to the bi-exponential ssHDX

kinetics are not yet clear, however. Therefore, we discuss differences among the formulations and processing methods studied here in terms of the experimental parameters of Eq. 1.

In S-SD and T-SD samples, the smaller values of  $N_{fast}$  (Table II) may be influenced by vapor diffusion through the powder. This effect is evident on comparing S-UCN and S-UCN-G samples, where  $N_{fast}$  in the ground lyophilized cake is significantly less than that in the intact cake.  $N_{slow}$ , however, was comparable in the trehalose samples (T-SD and T-UCN), and was even greater in S-SD samples than in S-UCN and S-CN, consistent with completion of mass transport through the powder at earlier time points. For mannitol samples, the mass transport effect appears to be overwhelmed by the large increase in  $N_{fast}$  in M-SD relative to M-UCN and M-CN samples (Table II).

In addition to differences in the extent and kinetics of ssHDX, various degrees of broadening in the deconvoluted mass envelopes of the deuterated samples were detected (Figs. 6 and 7). In solution HDX, peak broadening is expected during the deuteration time course as the extent of deuterium incorporation differs among the molecules in the sample (28). As deuteration nears completion in solution, the extent of deuteration becomes more uniform and peak broadening typically decreases (28). At a given extent of deuterium incorporation in solution HDX, peak broadening that exceeds that of a native control is consistent with a broadened distribution of protein conformations (27,28). Similarly, splitting of the mass envelope into two peaks at higher and lower  $m/z$  in solution HDX is consistent with the presence of two populations with different conformations. Here, we have applied these interpretations to peak broadening in ssHDX as well, with the proviso that not only protein conformation but also matrix interactions may be heterogeneous in samples that display increased peak broadening during exchange.

**Table II** Non-Linear Regression Parameters of Deuterium Uptake Kinetics (11% RH, RT) in the Intact mAb in Different Formulations

Formulation	$N_{fast}$	$k_{fast}$ ( $h^{-1}$ )	$N_{slow}$	$k_{slow}$ ( $h^{-1}$ )
M-SD	256 (16)	0.12(0.01)	131.5(24.44)	0.006(0.004)
M-UCN	180 (11)	0.18(0.02)	175.4(9.849)	0.009(0.002)
M-CN	158 (9)	0.18(0.02)	184.5(7.317)	0.012(0.002)
S-SD	41(20)	0.18(0.17)	167(17.3)	0.017(0.004)
S-UCN	88 (8)	0.21(0.04)	134.4(6.749)	0.012(0.002)
S-UCN-G	35(9)	0.18(0.04)	152.6(5.915)	0.019(0.003)
S-CN	65.61(8.428)	0.26(0.06)	149.5(7.444)	0.017(0.002)
T-SD	46(22)	0.13(0.06)	176(18.6)	0.015(0.003)
T-UCN	119.3(8.192)	0.19(0.03)	182.4(28.73)	0.006(0.002)
T-CN	NF	NF	NF	NF

See Eq. 1 and associated text for regression equation and parameter definitions. Values in parentheses represent standard errors of the regression parameters. NF indicates that an acceptable fit was not obtained

The peak broadening observed in the S-SD and T-SD samples suggests that there is a broader distribution of structural states in the spray dried powder than in the lyophilized cakes of sucrose and trehalose. The minor peak splitting observed in these samples (Fig. 6f–g) is consistent with the presence of two distinct populations. This may reflect heterogeneity in protein structure, since proteins are exposed to shear stress during atomization and high temperature during drying (2), with the mAb molecules at the interface with the atomizing and/or the drying gas are more vulnerable to structural perturbation than those in the particle core. Accumulation of a model mAb on the particle surface in spray dried powders has been shown to be greater than in lyophilized cakes (10). Therefore, it is possible that a significant fraction of the mAb in the S-SD and T-SD samples are present at the solid-air interface and may be structurally perturbed (29). Similar heterogeneity has recently been observed in spray dried trehalose and sucrose formulations using confocal fluorescence microscopy (30).

Peak broadening was also slightly greater in the CN than in the UCN samples for all excipients (Figs. 6 and 7). The similar extents of deuterium incorporation in these samples suggests that, while the ensemble average structural perturbation is similar for the two samples, the breadth of the distribution of these states is slightly greater for the CN samples. In a previous study, Iyer *et al.* (12) reported similar peak width/broadening in sucrose-containing formulations of myoglobin lyophilized using UCN or CN. However, in that study, ice nucleation was induced by pressurizing the chamber with an inert gas followed by rapid depressurization, whereas in the present study, ice nucleation was induced by introducing ice crystals into the pre-cooled vials. Typically, CN results in large sized ice crystals and hence less ice-solution interface, which would be expected to result in less denaturation and hence less conformational heterogeneity.

## CONCLUSIONS

The studies reported here assessed the effects of the drying process and formulation composition on the conformation and matrix interactions of an IgG1 mAb in solid samples. ssFTIR and fluorescence spectroscopies results show that the greatest structural perturbation occurred in mannitol samples, particularly those that were spray dried. The extent of ssHDX was greatest in all mannitol-containing formulations, and least in formulations containing sucrose. This suggests that the mannitol formulations are most structurally perturbed and/or have the fewest hydrogen bonding interactions between the protein and the surrounding matrix. Additionally, peak broadening in ssHDX-MS studies was greatest in spray dried samples of sucrose and trehalose, suggesting that the distribution of conformations was greatest in these samples. To our knowledge, the studies are the first use of ssHDX-MS methods

to assess the effects of spray drying on protein structure. The results demonstrate the sensitivity of the method to structural changes weakly indicated by or invisible to spectroscopic methods, and support the broader use of ssHDX-MS to measure formulation and process effects on protein structure in solid samples.

## ACKNOWLEDGMENTS AND DISCLOSURES

The IgG1 mAb used in this study was provided by Pfizer, Inc. (Chesterfield, MO). This work was supported in part by a Purdue Research foundation grant and a McKeehan Graduate Fellowship awarded by Purdue University to EM.

## REFERENCES

- Manning MC, Chou DK, Murphy BM, Payne RW, Katayama DS. Stability of protein pharmaceuticals: an update. *Pharm Res*. 2010;27(4):544–75.
- Walters RH, Bhatnagar B, Tchessalov S, Izutsu K, Tsumoto K, Ohtake S. Next generation drying technologies for pharmaceutical applications. *J Pharm Sci*. 2014;103(9):2673–95.
- Wang W. Lyophilization and development of solid protein pharmaceuticals. *Int J Pharm*. 2000;203(1–2):1–60.
- Searles JA, Carpenter JF, Randolph TW. The ice nucleation temperature determines the primary drying rate of lyophilization for samples frozen on a temperature-controlled shelf. *J Pharm Sci*. 2001;90(7):860–71.
- Geidobler R, Winter G. Controlled ice nucleation in the field of freeze-drying: fundamentals and technology review. *Eur J Pharm Biopharm*. 2013;85(2):214–22.
- Cicerone MT, Pikal MJ, Qian KK. Stabilization of proteins in solid form. *Adv Drug Deliv Rev*. 2015;93:14–24.
- Ohtake S, Kita Y, Arakawa T. Interactions of formulation excipients with proteins in solution and in the dried state. *Adv Drug Deliv Rev*. 2011;63(13):1053–73.
- Awotwe-Otoo D, Agarabi C, Read EK, Lute S, Brorson KA, Khan MA. Product and process understanding to relate the effect of freezing method on glycation and aggregation of lyophilized monoclonal antibody formulations. *Int J Pharm*. 2015;490(1–2):341–50.
- Parker A, Rigby-Singleton S, Perkins M, Bates D, Le Roux D, Roberts CJ, *et al*. Determination of the influence of primary drying rates on the microscale structural attributes and physicochemical properties of protein containing lyophilized products. *J Pharm Sci*. 2010;99(11):4616–29.
- Abdul-Fattah AM, Truong-Le V, Yee L, Nguyen L, Kalonia DS, Cicerone MT, *et al*. Drying-induced variations in physico-chemical properties of amorphous pharmaceuticals and their impact on stability (I): stability of a monoclonal antibody. *J Pharm Sci*. 2007;96(8):1983–2008.
- Sane SU, Wong R, Hsu CC. Raman spectroscopic characterization of drying-induced structural changes in a therapeutic antibody: correlating structural changes with long-term stability. *J Pharm Sci*. 2004;93(4):1005–18.
- Iyer LK, Sacha GA, Moorthy BS, Nail SL, Topp EM. Process and formulation effects on protein structure in lyophilized solids using mass spectrometric methods. *J Pharm Sci*. 2016;105(5):1684–92.
- Moorthy BS, Iyer LK, Topp EM. Mass spectrometric approaches to study protein structure and interactions in lyophilized powders. *J Vis Exp*. 2015(98).
- Moorthy BS, Zarraga IE, Kumar L, Walters BT, Goldbach P, Topp EM, Allmendinger A. Solid-state hydrogen–deuterium exchange mass spectrometry: correlation of deuterium uptake and long-term stability of lyophilized monoclonal antibody formulations. *Mol Pharm*. 2017. <https://doi.org/10.1021/acs.molpharmaceut.7b00504>.
- Sophocleous AM, Zhang J, Topp EM. Localized hydration in lyophilized myoglobin by hydrogen-deuterium exchange mass spectrometry. 1. Exchange mapping. *Mol Pharm*. 2012;9(4):718–26.
- Fu F, DeOliveria D, Trumble W, Sakar B, Singh B. Secondary structure estimation of proteins using the amide III region of Fourier transform infrared spectroscopy. Application to analyse calcium binding-induced structural changes in calsequestrin. *Appl Spectrosc*. 1994;48:1432–41.
- Kelly SM, Jess TJ, Price NC. How to study proteins by circular dichroism. *Biochim Biophys Acta*. 2005;1751(2):119–39.
- Sharma VK, Kalonia DS. Steady-state tryptophan fluorescence spectroscopy study to probe tertiary structure of proteins in solid powders. *J Pharm Sci*. 2003;92(4):890–9.
- Ramachander R, Jiang Y, Li C, Eris T, Young M, Dimitrova M, *et al*. Solid state fluorescence of lyophilized proteins. *Anal Biochem*. 2008;376(2):173–82.
- Schule S, Friess W, Bechtold-Peters K, Garidel P. Conformational analysis of protein secondary structure during spray-drying of antibody/mannitol formulations. *Eur J Pharm Biopharm*. 2007;65(1):1–9.
- Chang L, Shepherd D, Sun J, Ouellette D, Grant KL, Tang XC, *et al*. Mechanism of protein stabilization by sugars during freeze-drying and storage: native structure preservation, specific interaction, and/or immobilization in a glassy matrix? *J Pharm Sci*. 2005;94(7):1427–44.
- Park J, Nagapudi K, Vergara C, Ramachander R, Laurence JS, Krishnan S. Effect of pH and excipients on structure, dynamics, and long-term stability of a model IgG1 monoclonal antibody upon freeze-drying. *Pharm Res*. 2013;30(4):968–84.
- Souillac PO, Middaugh CR, Rytting JH. Investigation of protein/carbohydrate interactions in the dried state. 2. Diffuse reflectance FTIR studies. *Int J Pharm*. 2002;235(1–2):207–18.
- Englander SW, Mayne L, Bai Y, Sosnick TR. Hydrogen exchange: the modern legacy of Linderström-Lang. *Protein Sci Publ Protein Soc*. 1997;6(5):1101–9.
- Li Y, Williams TD, Schowen RL, Topp EM. Characterizing protein structure in amorphous solids using hydrogen/deuterium exchange with mass spectrometry. *Anal Biochem*. 2007;366(1):18–28.
- Moorthy BS, Schultz SG, Kim SG, Topp EM. Predicting protein aggregation during storage in lyophilized solids using solid state amide hydrogen/deuterium exchange with mass spectrometric analysis (ssHDX-MS). *Mol Pharm*. 2014;11(6):1869–79.
- Sophocleous AM, Topp EM. Localized hydration in lyophilized myoglobin by hydrogen-deuterium exchange mass spectrometry. 2. Exchange kinetics. *Mol Pharm*. 2012;9(4):727–33.
- Weis DD, Wales TE, Engen JR, Hotchko M, Ten Eyck LF. Identification and characterization of EX1 kinetics in H/D exchange mass spectrometry by peak width analysis. *J Am Soc Mass Spectrom*. 2006;17(11):1498–509.
- Hsu CC, Nguyen HM, Yeung DA, Brooks DA, Koe GS, Bewley TA, *et al*. Surface denaturation at solid-void interface—a possible pathway by which opalescent particulates form during the storage of lyophilized tissue-type plasminogen activator at high temperatures. *Pharm Res*. 1995;12(1):69–77.
- Koshari SH, Ross JL, Nayak PK, Zarraga IE, Rajagopal K, Wagner NJ, *et al*. Characterization of protein-excipient microheterogeneity in biopharmaceutical solid-state formulations by confocal fluorescence microscopy. *Mol Pharm*. 2017;14(2):546–53.